



HAL
open science

The role of peroxiredoxin 6 in biosynthesis of FAHFAs

Veronika Paluchova, Tomas Cajka, Thierry Durand, Claire Vigor, Chandra Dodia, Shampa Chatterjee, Aron Fisher, Ondrej Kuda

► **To cite this version:**

Veronika Paluchova, Tomas Cajka, Thierry Durand, Claire Vigor, Chandra Dodia, et al.. The role of peroxiredoxin 6 in biosynthesis of FAHFAs. *Free Radical Biology and Medicine*, 2022, 193 (Part 2), pp.787-794. 10.1016/j.freeradbiomed.2022.11.015 . hal-03870277

HAL Id: hal-03870277

<https://hal.science/hal-03870277>

Submitted on 25 Nov 2022

HAL is a multi-disciplinary open access archive for the deposit and dissemination of scientific research documents, whether they are published or not. The documents may come from teaching and research institutions in France or abroad, or from public or private research centers.

L'archive ouverte pluridisciplinaire **HAL**, est destinée au dépôt et à la diffusion de documents scientifiques de niveau recherche, publiés ou non, émanant des établissements d'enseignement et de recherche français ou étrangers, des laboratoires publics ou privés.

The Role of Peroxiredoxin 6 in Biosynthesis of FAHFAs

Veronika Paluchova^{1,2}, Tomas Cajka¹, Thierry Durand³, Claire Vigor³, Chandra Dodia⁴, Shampa Chatterjee⁴, Aron B. Fisher⁴, Ondrej Kuda¹

¹ Institute of Physiology of the Czech Academy of Sciences, Videnska 1083, 14220 Prague 4, Czech Republic

² First Faculty of Medicine, Charles University, Katerinska 32, Prague 12108, Czech Republic

³ Institut des Biomolécules Max Mousseron, CNRS, ENSCM, University Montpellier, 34093 Montpellier, France

⁴ Institute for Environmental Medicine of the Department of Physiology, University of Pennsylvania, 3620 Hamilton Walk, 1 John Morgan Building, USA

1 ABSTRACT

Peroxiredoxin 6 (Prdx6) is a multifunctional enzyme, a unique member of the peroxiredoxin family, with an important role in antioxidant defense. Moreover, it has also been linked with the biosynthesis of anti-inflammatory and anti-diabetic lipids called fatty acid esters of hydroxy fatty acids (FAHFAs) and many diseases, including cancer, inflammation, and metabolic disorders. Here, we performed lipidomic profiling of subcutaneous adipose from mouse models with genetically modified Prdx6. Deletion of Prdx6 resulted in reduced levels of FAHFAs containing 13-hydroxylinoleic acid (13-HLA). Mutation of Prdx6 C47S impaired the glutathione peroxidase activity and reduced FAHFA levels while D140A mutation, responsible for phospholipase A2 activity, showed only minor effects. Targeted analysis of oxidized phospholipids and triacylglycerols in adipocytes highlighted a correlation between FAHFA and hydroxy fatty acid production by Prdx6. FAHFA regioisomer abundance was negatively affected by the Prdx6 deletion, and this effect was more pronounced in longer and more unsaturated FAHFAs. The predicted protein model of Prdx6 suggested that the monomer-dimer transition mechanism might be involved in the preferred repair of longer peroxidized phospholipids, which were bound over two monomers. In conclusion, our work linked the peroxidase activity of Prdx6 with the levels of FAHFAs in adipose tissue.

2 ABBREVIATIONS

FAHFA – fatty acid ester of hydroxy fatty acid

POHLA – palmitoleic acid ester of hydroxy linoleic acid

HFA – hydroxy fatty acid

(H)PA – (hydroxy) palmitic acid

(H)PO – (hydroxy) palmitoleic acid

(H)SA – (hydroxy) stearic acid

(H)OA – (hydroxy) oleic acid

(H)LA – (hydroxy) linoleic acid

(H)AA – (hydroxy) arachidonic acid

(H)DHA – (hydroxy) docosahexaenoic acid

HODE – hydroxy octadecadienoic acid

LPC – lysophosphatidylcholine

PE – phosphatidylethanolamine

PC – phosphatidylcholine

TAG – triacylglycerol

3 INTRODUCTION

During conditions of oxidative stress, reactive oxygen species (ROS) readily attack phospholipids (PLs), which results in their peroxidation and consequently leads to disruption of the membrane

lipid bilayer arrangement [1]. Peroxiredoxin 6 (Prdx6), also called 1-Cys peroxiredoxin (UniProt ID O08709), exists as a dimer and it is the last identified mammalian enzyme of the peroxiredoxin family [2, 3]. It has been assumed to play an important role in several health disorders, including acute lung injury and inflammation [4-6], type 1 diabetes [7], male fertility [8], cancer [9, 10], and ferroptosis, which is highly related to cancer [11]. The mechanism of the catalytic activity is based on a single active cysteine, in contrast to a 2-cys mechanism common for most other members of the peroxiredoxin family. The fact that Prdx6 uses glutathione (GSH) rather than thioredoxin as a reducing agent for peroxidase activity [2, 12], makes Prdx6 a unique member of the peroxiredoxin family. It also plays a crucial role in antioxidant defense as it can bind to peroxidized phospholipids (PLOOHs) and repair them through its enzymatic activities [12, 13] (Figure 1A). Three enzymatic activities of Prdx6 have been described: a) glutathione peroxidase activity, b) phospholipase A₂ (PLA₂) activity, and c) lysophosphatidylcholine acyltransferase (LPCAT) activity.

3.1 Peroxidase activity

Prdx6 can reduce peroxidized phospholipids to the corresponding alcohols (PLOHs) through its peroxidase activity, which involves three main steps: peroxidation, resolution, and recycling. Peroxidation reduces hydroperoxides through the single conserved cysteine oxidation to a sulfenic form. The following resolution uses an external reducing agent, glutathione (GSH), namely the π isoform of the enzyme GSH S-transferase (π GST) as Prdx6 does not have a second resolving cysteine, resulting in glutathionylated Prdx6. Then it reacts with free GSH to return to a fully reduced state in a process called recycling [3, 14, 15]. The phospholipid hydroperoxidase GSH peroxidase (PHGPx) activity is dependent on catalytic cysteine (Cys) at position 47 (C47). Mutating cysteine to serine (C47S) abolishes the ability of Prdx6 to reduce hydroperoxides but does not affect PLA₂ activity [16, 17] (Figure 1B).

3.2 Phospholipase A2 activity

Prdx6 is the only member of the Prdx family that possesses phospholipase A₂ (PLA₂) activity, which also participates in the phospholipid turnover by hydrolyzing an oxidized fatty acid (FA) bound at the *sn*-2 position, thus generating lysoPLs [3, 18]. It is a calcium-independent activity and requires a catalytic triad serine at position 32 (S32), histidine at position 26 (H26), and aspartate at position 140 (D140). Since H26 and S32 are necessary for binding Prdx6 to the phospholipid, a mutation of aspartate to alanine (D140A) was found to be the most suitable one for abolishing the PLA₂ activity [19, 20] (Figure 1B).

3.3 Lysophosphatidylcholine acyltransferase activity

Lysophosphatidylcholine acyltransferase (LPCAT) activity is coupled to the PLA₂ activity and re-acylates the *sn*-2 position of lysoPLs with a FA-CoA. This activity generates remodeled phosphatidylcholine (PC) and is important for dipalmitoylphosphatidylcholine lung surfactant [3, 13].

3.4 Biosynthesis of FAHFA

A previous study linked Prdx6 with the biosynthesis of FAHFAs (fatty acid esters of hydroxy fatty acids) via QTL mapping, suggesting that PLOH, generated during the process of peroxidized phospholipid repair, could serve as a source of the hydroxy fatty acid (HFA) in FAHFA structure [21]. FAHFAs represent a diverse group of lipids. The position of the ester bond between the HFA and the (FA) defines the regioisomer and also the biological activities, mainly anti-diabetic and anti-

inflammatory [22, 23]. A review summarizing current knowledge about their metabolism, biological effects, and synthesis has been recently published [24].

Here, we present a study exploring the effects of specific enzymatic activities of Prdx6 on FAHFA levels. We hypothesize that the glutathione peroxidase activity is important for the generation of HFA for FAHFA synthesis. For this purpose, we used mouse models with genetically altered Prdx6: one knock-out model (Prdx6 null), two knock-in models (C47S, D140A), and wild-type (WT) mice as a control group.

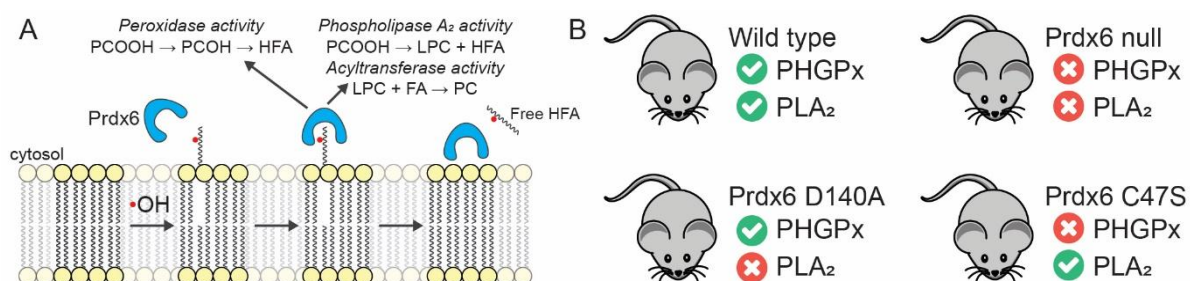


Figure 1. Illustrative overview (A) Scheme of the function of Prdx6 and its enzymatic activities. Adapted from Manevich, 2009 [25]. (B) Overview of mouse models used in the study – wild-type mice and mice with genetically altered Prdx6 (Prdx6 null, D140A, and C47S).

4 MATERIALS AND METHODS

4.1 Materials and Reagents

LC–MS-grade solvents and mobile phase modifiers were purchased from VWR International (Czech Republic). FAHFA standards were from Cayman Europe (Tallinn, Estonia), and all other chemicals, including selective Glutathione peroxidase 4 (GPX4) inhibitor (ML210), were ordered from Merck (Czech Republic) unless stated otherwise. GPX4 functions as a phospholipid hydroperoxidase to reduce phospholipid hydroperoxide (20:4- or 22:4-PE-OOH) to the corresponding phospholipid alcohol (PLOH) [26]. MJ33 is an inhibitor of the PLA₂ activity of Prdx6 [27].

4.2 Animal Studies

Mouse models (Prdx6 null, Prdx6 D140A, and C47S knock-in mice) used in this study were bred in animal care facilities of the Institute for Environmental Medicine, Department of Physiology, Perelman School of Medicine of the University of Pennsylvania. The generation of these mouse models has been described previously [28]. Wild-type mice C57Bl/6 were obtained from the Jackson Laboratory (Bar Harbor, ME). We used male and female mice 10-13 weeks old in this study. Mice were maintained at 22 °C on a 12h light/dark cycle while feeding a standard chow diet and having unlimited access to water. Mice were fasted for 24 hours and then re-fed overnight with 15% sucrose in drinking water before scarification to stimulate de novo lipogenesis. All tissue samples (subcutaneous white adipose tissue (scWAT) and the liver)) were collected into cryovials, immediately frozen in liquid nitrogen, and stored at – 80 °C freezer. The University of Pennsylvania Animal Care and Use Committee (IACUC) approved all procedures involving mice.

4.3 Cell Culture experiments

The 3T3-L1 cell line was differentiated according to the standard protocol [29]. Differentiated adipocytes were incubated in a DMEM complete medium (25 mmol/L glucose, 10% FBS, 850 nmol/L insulin, penicillin/streptomycin) supplemented with a 40 μM mixture of polyunsaturated FAs (OA, LA, AA, DHA; 10 μM each, complexed to BSA at the ratio 3:1) for 96 hours to provide building blocks

for more complexed FAHFAs. For the last 24 hours, inhibitors MJ33 and ML210 were added to the medium (10 μ M) separately or combined to mimic the Prdx6 null mouse model.

4.4 Sample processing

Tissue samples were divided into aliquots in liquid nitrogen and three different extraction protocols and LC-MS analyzes were applied. Liquid nitrogen or ice was used during sample processing to prevent the degradation of oxidized PLs (PLOOHs, PLOHs). All samples were used for lipidomic profiling and targeted methods including FAHFA analysis. Only the liver samples were used to measure isoprostanes (IsoP) as oxidative stress biomarkers due to limited sample amounts.

4.4.1 FAHFA analysis

FAHFAs extraction was based on liquid-liquid extraction followed by solid-phase extraction performed according to the published methods [22, 30]. The final dried and purified extract was re-suspended in methanol and immediately analyzed using an UltiMate 3000 RSLC UHPLC system coupled to a QTRAP 5500/SelexION mass spectrometer (SCIEX, Darmstadt, Germany) with Triart C18 ExRS 250 \times 2.0 mm; 3 μ m column (YMC, Japan). FAHFAs were detected in negative ESI mode as before [29].

4.4.2 Lipidomic profiling and targeted analysis

Nonpolar analytes were extracted using a mixture of cold water, methanol, and methyl *tert*-butyl ether (MTBE), as published before, with some modifications [31, 32]. A Vanquish UHPLC System (Thermo Fisher Scientific, Bremen, Germany) coupled to a Q Exactive Plus mass spectrometer (Thermo Fisher Scientific, Bremen, Germany) together with LIMeX (Lipids, Metabolites, and eXposome compounds) LC-MS workflow was used for the untargeted analysis of complex lipids and polar metabolites [33]. Parallel Reaction Monitoring (PRM) mode and inclusion lists were used to identify and measure oxidized phospholipids.

4.4.3 Isoprostane analysis

Extraction of IsoPs was based on a published protocol [34] with certain modifications for the liver. Liver tissue (200 mg) was mixed with 50 μ L of BHT (1% in ethanol) and 1 mL of a cold mixture of methanol and 5 mM EGTA in water (2:1) and spiked with 5 ng of each internal standard. The mixture was homogenized using a Fast Prep instrument (MP Biomedicals) for 30 s at 6.5 m/s. After transferring the homogenate into a new tube, the rest was re-extracted by adding cold methanol (830 μ L) and phosphate buffer (800 μ L). Finally, after the addition of cold chloroform (3 mL) to perform Folch extraction, the mixture was vortexed (30 s) and centrifuged (2,000 \times g, 5 min, 4 $^{\circ}$ C). The lower organic phase was carefully transferred in a Pyrex tube and dried under a flow of nitrogen (40 $^{\circ}$ C, 30 min). Then, extracted lipid fraction was hydrolyzed with 1 M KOH in methanol (0.95 mL) and incubated for 30 min at 40 $^{\circ}$ C while rotating. After cooling to room temperature, we added 2 mL of 40 mM formic acid and further extracted samples by SPE (OASIS MAX 200 mg, 3 mL). SPE columns were cleaned with methanol (2 mL) and conditioned with 2 mL of 20 mM of formic acid. After loading the samples, SPE columns were washed in several steps: 1) 2% NH₄OH (2 mL), 2) 20 mM formic acid/methanol (70:30, v/v) (2 mL), 3) hexane (2 mL), and 4) hexane/ethyl acetate (70:30, v/v), (2 mL). The IsoPs were eluted with 2 mL of a mixture of hexane/ethanol/acetic acid (70:29.4:0.6, v/v/v), dried under a flow of nitrogen at 40 $^{\circ}$ C, resuspended in 100 μ L of water/acetonitrile (87:17, v/v), centrifuged through a filter (10,000 \times g, 1 min, RT) and transferred in a plastic injection vial. An Eksigent microLC 200 Plus system coupled to a QTRAP 5500 (Sciex, Darmstadt, Germany) was used to analyze IsoPs [35].

4.5 Prdx6 protein model

ColabFold pipeline v1.3 including MMseqs2 with AlphaFold2-multimer engine (databases UniRef30 2022_02 and PDB/PDB70 220313) was used to predict human Prdx6 dimer model (Uniprot # P30041, reduced form) [36]. ChimeraX v1.4 (VinaDock v1.2) was used to dock the oxidized phosphatidylcholine (PC 16:0/13(S)-HpODE) ligand [37]. 13(S)-HpODE (13-(S)-hydroperoxyoctadecadienoic acid) is the most abundant peroxidized metabolite of LA. The PDB model is included in SI material (Figure Sx and ZIP).

4.6 Data Processing and Statistics

LC-MS data from the LIMeX workflow were processed using MS-DIAL ver. 4.70 [32]. Metabolites were annotated using in-house retention time–*m/z* library and using MS/MS libraries available from public sources (MassBank, MoNA). Raw data were filtered using blank samples, serial dilution samples, and quality control (QC) pool samples with relative standard deviation (RSD) < 30%, and then normalized using the LOESS approach by means of QC pool samples for each matrix regularly injected between 10 actual samples. LC-MS/MS data from targeted analysis of FAHFAs and IsoPs were processed using MultiQuant software (SCIEX). Data were further processed via MetaboAnalyst [38] and GraphPad Prism to compare groups (Student *t*-test, *p* < 0.05 was considered significant). Lipid enrichment was calculated as before [39].

5 RESULTS

5.1 Mild effect of Prdx6 deletion on scWAT lipidome

We explored the role of Prdx6 in scWAT lipid metabolism. We used a mouse model of *Prdx6* deletion (global knockout), *Prdx6* C47S, and D140A knock-in mice to target the particular enzymatic activities. Deletion of *Prdx6* resulted in mild changes of the scWAT lipidome and we did not find any specific pattern in the downregulated lipids but enrichment in FA 18:2 (Figure 2A). Mice harboring the C47S mutation showed several downregulated and upregulated lipid species. Downregulated cluster was enriched in short chain TAG species containing saturated FAs with 8-14 carbons. The upregulated lipid cluster was characterized by ether phosphatidylethanolamines (PE) containing mainly O-20:1 acyl chains and steroid sulfate conjugates (Figure 2B). The D140A mutation showed the weakest effect compared to wild type mice and only a few steroid sulfate conjugates were upregulated (Figure 2C). Based on the original hypothesis, we focused only on the lipids related to oxidation and FAHFA synthesis.

5.2 Oxidative stress markers were unaltered by deletion of Prdx6

Next, we checked the markers of oxidative stress. Levels of reduced glutathione in scWAT were similar between all genotypes and only the oxidized glutathione was increased in C47S mutation (Figure 2D). The marker of susceptibility to ferroptosis (PE O-16:1/20:4) was not altered in scWAT (Figure 2E) and the levels of isoprostanes did not suggest oxidative stress condition in the liver (Figure 2F). Therefore, we concluded that the missing Prdx6 enzymatic activities were compensated

by other general antioxidant mechanisms.

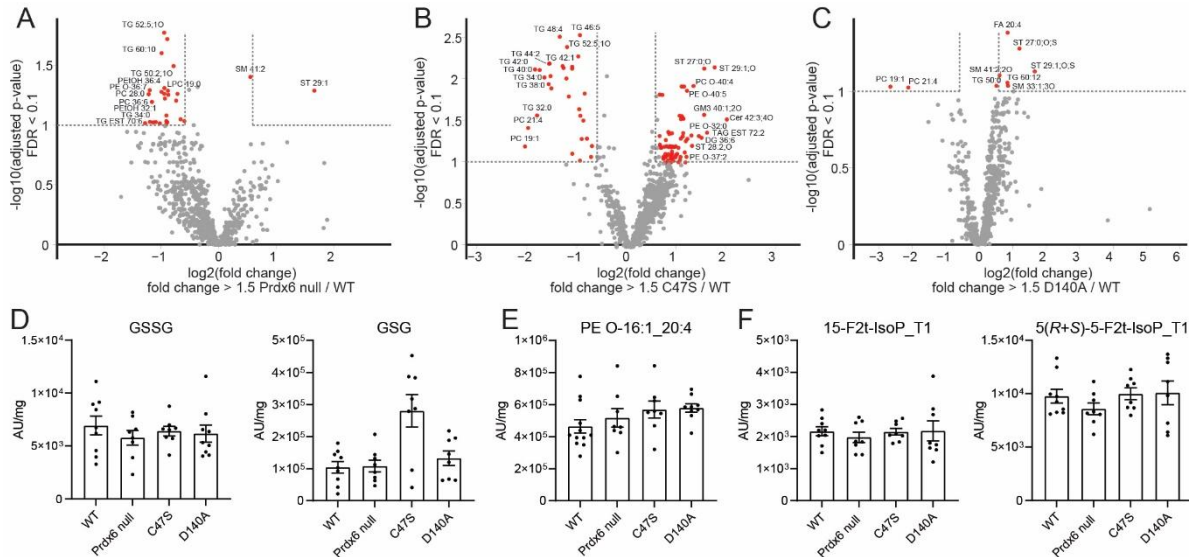


Figure 2: scWAT lipidome alterations. (A) Volcano plot comparing Prdx6 null mice and wild type mice (WT). Metabolites with fold change > 1.5 and FDR < 0.1 were highlighted in red. (B) Volcano plot for C47S and WT. (C) Volcano plot for D140A and WT. (D) Levels of reduced and oxidized glutathione in scWAT. (E) Levels of PE-O 16:1/20:4 in scWAT. (F) Levels of isoprostanes in the liver. Data are mean \pm S.E., $n = 8-9$.

5.3 Putative pathway of FAHFA biosynthesis

Lipids downregulated in Prdx6 null mice contained linoleic acid (FA 18:2). Therefore, we explored the levels of highly abundant FAHFAs containing 13-hydroxylinoleic acid (HLA or 18:2;O chain). Scheme in Figure 3A illustrated the putative metabolic pathway of FAHFA synthesis. Oxidized membrane phospholipids serve as a source of hydroxylated FAs which are then incorporated into TAGs. The ATGL biosynthetic transacylase activity combines two TAGs and creates a TAG estolide (TG-FAHFA). Free FAHFAs are liberated from TAG estolides by HSL or CEL [39-41] (Figure 3A). Levels of 13-HLA-containing FAHFAs were significantly downregulated in Prdx6 null scWAT and this effect was also observed also in C47S mice. The lack of PLA₂ activity in D140A mice had the weakest effect on FAHFA levels. Interestingly, the longer and more unsaturated FAHFAs were affected more than the shorter and saturated species (Figure 3B). The untargeted lipidomic analysis also showed several TAG species containing HLA, which could be the intermediates in FAHFA synthesis (Figure 3C). Their profiles were similar to the FAHFA profiles.

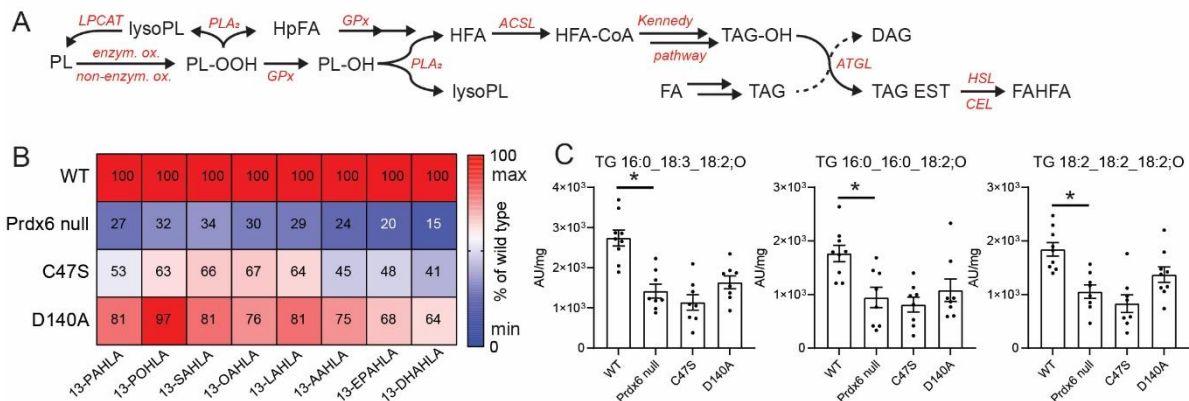


Figure 3: FAHFA synthesis in scWAT. (A) Proposed scheme of FAHFA synthesis. ATGL, adipose triglyceride lipase; CEL, carboxyl ester lipase; DAG, diacylglycerol; FA, fatty acid; GPx, peroxidase

activity; HFA, hydroxy fatty acid, e.g. 13-HLA; HpFA, hydroproxy FA; HSL, hormone-sensitive lipase; LPCAT, acyltransferase activity; lysoPL, lysophospholipid; PLA2, phospholipase A2 activity; PL, phospholipid, e.g. PC; PL-OH, hydroxylated PC; PL-OOH, peroxidated PL; TAG, triacylglycerol; TAG EST, triacylglycerol estolide (TG-FAHFA). (B) Levels of FAHLA (containing 13-HLA) in scWAT expressed as percentage of wild type (WT) group. (C) Levels of TAGs containing hydroxylated 18:2 (HLA in general) in scWAT. Data are mean \pm S.E., $n = 8-9$, * significantly different at $p < 0.05$.

The untargeted lipidomic profiling cannot capture the peroxidized phospholipid species (putative intermediates in HFA synthesis). Therefore, we performed the targeted analysis using 3T3-L1 adipocytes exposed to ML210 (inhibitor of phospholipid peroxidase activity) and or MJ33 (inhibitor of PLA₂ activity of Prdx6). This situation mimicked the animal models (Figure 1). We selected the PC 16:0/18:2 as the tracer molecule. Peroxidized PC 16:0/18:2;2O and hydroxylated PC 16:0/18:2;O showed profiles that resembled the pattern observed in mouse scWAT (Figure 4A). Levels of 13-HLA were downregulated only by the combination of both inhibitors (Figure 4B), while the levels of HLA-containing FAHFAs were similar to the animal profiles (Figure 4C and Figure 3). The animal and in vitro data suggest that Prdx6 participates in FAHFA biosynthesis and that peroxidase activity is the main enzymatic activity of Prdx6 involved in this process.

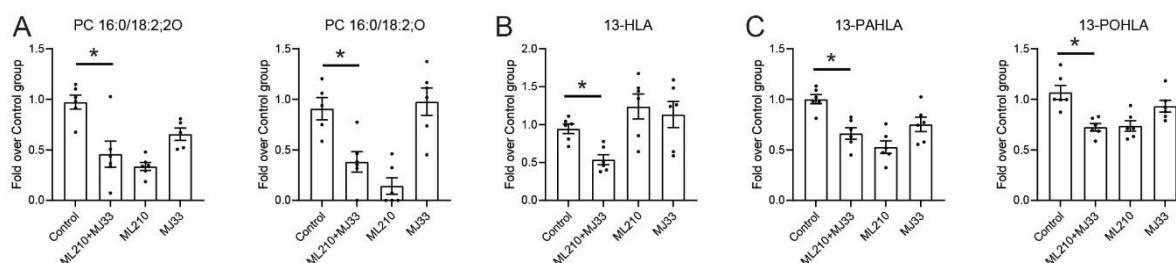


Figure 4: Targeted analysis of 3t3-L1 cells. (A) Levels of peroxidized and oxidized (hydroxylated) PC 16:0/18:2. (B) Levels of 13-HLA (FA 18:2;O). (C) FAHFA levels. Data are mean \pm S.E., $n = 8-9$, * significantly different at $p < 0.05$.

5.4 Prdx6 deletion affects FAHFA regioisomer abundance

To explore Prdx6 regioselectivity and substrate specificity affecting potential FAHFA precursors, we explored FAHFAs with different branching positions, chain lengths, and saturation levels of HFAs. The branching position and the type of HFA were dependent on Prdx6 presence (Figure 5). The further was the hydroxyl group from an α -carbon atom of HFA, the more significant was the effect of Prdx6 deletion on FAHFA levels (Figure 5A and Figure 5B). The palmitic acid and oleic acid chains were kept constant for each profile. We observed this effect also for saturated FAHFAs (Figure 5C), although Prdx6 deletion negatively affected levels of unsaturated FAHFA more than those of saturated FAHFAs (Figure 5 and Figure 2).

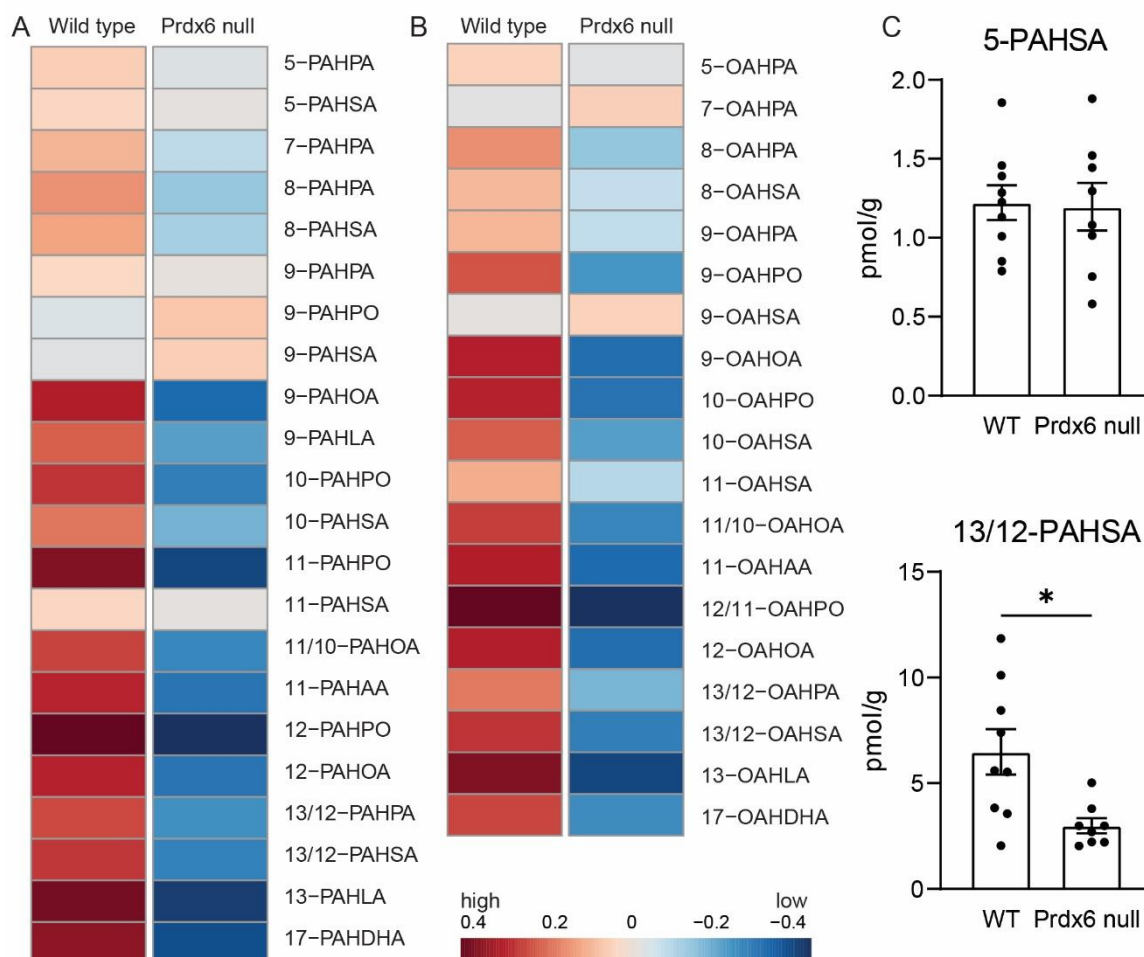


Figure 5: FAHFA regioisomers in scWAT. (A) Heatmap of FAHFA regioisomers containing palmitic acid (PA) and different HFAs with 16 to 22 carbon atoms. (B) Heatmap of FAHFA regioisomers containing oleic acid (OA) and different HFAs with 16 to 22 carbon atoms. (C) Regioisomers of saturated FAHFA. * Statistically different at $p < 0.05$ by Student t -test comparing Prdx6 null vs. WT.

5.5 Prdx6 protein model

Prdx6's activity is conformation driven process which involves monomer–dimer transition [42]. To visualize the process and the key amino acid residues, we used AlphaFold2-multimer algorithm implemented as ColabFold pipeline to predict Prdx6 dimer structure [36]. Next, we used ChimeraX to dock an oxidized PC ligand (PC 16:0/13(S)-HpODE) and explore the putative active sites [37] (Figure 6A). The prediction showed that two monomers created a deep valley at their interface to fit the oxidized 13(S)-HpODE chain close to the peroxidatic Cys47 residue (Figure 6A and 6B). Simultaneously, the glycerol backbone and the ester bonds were positioned close to the Asp140 residue, important for the PLA₂ activity, on the flat surface of the protein [20]. While the peroxidase activity was localized within the monomer B, the PLA₂ activity residues were localized within the A chain (Figure 6C). This confirms the monomer-dimer transition mechanism and the proposed phospholipid binding over two monomers [43]. It also partially explained the effect on regioisomer branching position (Figure 5) when the peroxidation at carbon atoms further from the α -carbon can be more easily processed by Prdx6 peroxidase activity.

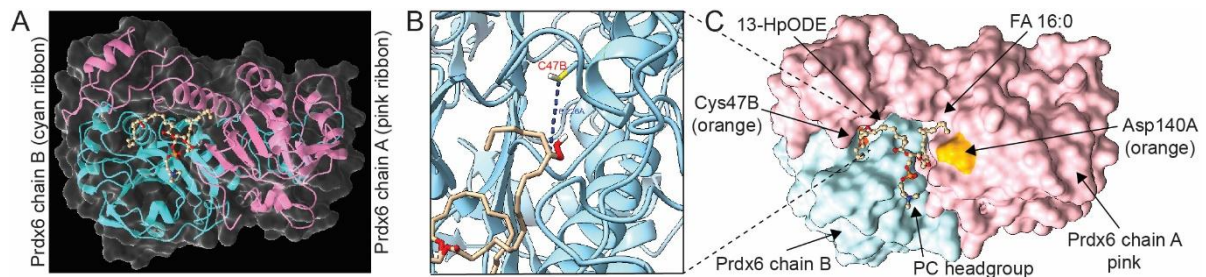


Figure 6. Model of Prdx6 dimer. (A) Chain A in pink and chain B in cyan within the transparent protein surface. Ligand PC 16:0/18:2;2O is shown as balls & sticks model. (B) Detail of the active site within chain B. The distance between carbon number 13 in 13(S)-HpODE and thiol group of C47B is approx. 6.2 Å. (C) Annotated surface structure of the Prdx6 dimer.

6 DISCUSSION

Elucidation of FAHFA metabolism has been one of the main goals since their discovery in 2014 [22]. The synthesis of FAHFAs, FAHFA storage, degradation and metabolic regulations [40, 41, 44, 45] have been described and summarized in a review [46]. However, the mechanism of HFA synthesis has not been fully elucidated yet. Here, we report the role of the glutathione peroxidase activity of Prdx6 in the biosynthesis of FAHFA.

Lipidomic profiling of mouse models showed that whole body Prdx6 knockout had only a mild impact on the general lipidome of scWAT. We did not observe any massive increase of oxidized lipids, but the targeted methods highlighted that levels of specific oxidized lipids were in fact lower in Prdx6 null mice. We speculate that the antioxidant defense system for lipids, mainly GPX4, compensated the loss of Prdx6 in scWAT and that only Prdx6-specific role was dysregulated. This is supported by the unaltered oxidative stress and ferroptosis susceptibility markers.

The knock-in model C47S showed more dysregulated scWAT lipidome than the Prdx6 knockout and the D140A model was nearly identical to wild type mice. The physical presence of mutated Prdx6 protein might participate in the signaling cascades and the effect of the mutation could be more pronounced in the tissues that are primarily under oxidative stress, e.g. lungs.

The cluster of downregulated lipids in Prdx6 null mice highlighted altered metabolism of FA 18:2. We explored FAHFAs containing HLA, specifically the most abundant 13-HLA, and found significantly lower levels in Prdx6 null mice. C47S mouse model confirmed that the peroxidase activity is linked to FAHFA levels while the PLA₂ is dispensable. Next, we explored the putative metabolic intermediates in the synthesis of FA-HLAs, the hydroxy TAGs containing 13-HLA, and found the same concentration patterns. In general, the hydroxy-TAGs should be used by ATGL to generate TAG estolides [40]. However, this neutral lipid remodeling process creates a huge number of isomeric structures (TAG *sn* position, FAHFA regioisomers) and acyl combinations (FAHFA and two FAs) [41]. There is currently no analytical approach for this challenge and we detected only pooled signals for TAG estolide families that are approximately 100-times more concentrated than the free FAHFAs [45]. Therefore, we could not track the fate of hydroxy-TAGs any further.

To explore the other branch of FAHFA synthesis, we focused on oxidized PCs, which are the preferred substrates of Prdx6 [47]. We used a cell culture model of adipocytes to precisely control the extraction procedure of oxidized lipids and a combination of inhibitors to mimics the mouse models. The levels of peroxidized PC 16:0/18:2;2O, hydroxylated PC 16:0/18:2;O, and 13-HLA-containing FAHFA showed similar profiles to FAHFAs which we previously detected in mice. This suggests a mechanistic link between Prdx6 peroxidase activity and FAHFA levels. Although the expected effects of Prdx6 deletion or inhibition in mice and cells could be the increase of (per)oxidized lipids, we observed the opposite. We could speculate that the antioxidant system in

adipose tissue compensated the loss of Prdx6 action and degraded the oxidized lipids [48], while the alternative pathway storing oxidized acyls within lipid droplets was scaled down [49]. The adipose tissue could store the oxidized lipids in lipid droplets in a form of oxidized TAGs or in lipid droplet surface phospholipid monolayer, and therefore provide the substrates for TAG estolide synthesis. Inhibition of this process could limit the availability of hydroxy-TAGs and further affect FAHFA levels.

Reduced levels of 13-HLA-containing FAHFAs in scWAT were dependent on the length and saturation of the FAHFA chain and a similar effect was observed for PA- an OA-containing FAHFAs, respectively. The protein model of Prdx6 dimer and Figure 5 heatmaps suggested that the peroxidase active residue Cys47 can repair oxidized carbon atoms from the position nine further to the tail of the PC acyl chain. The specific distribution of acyl composition in PCs and TAGs, adipose tissue depot and feeding status might affect the biosynthesis of FAHFAs within lipid remodeling cycle [21, 30, 40, 41, 44].

In conclusion, our work linked the peroxidase activity of Prdx6 with the levels of FAHFAs in adipose tissue. The fate of oxidized acyl chains within lipid remodeling cycle, specificity of the enzymatic machinery, and the co-regulation with antioxidant defense system remains unknown for future research.

7 Duality of Interest

The authors declare that there are no competing interests associated with the manuscript.

8 Funding

This work was supported by a grant from the Ministry of Education, Youth and Sports of the Czech Republic (LTAUSA18104).

9 Acknowledgment

Conceptualization: A.B.F. and O.K.; Data curation: V.P.; Formal analysis: V.P., T.C. and O.K.; Funding acquisition: T.D., A.B.F. and O.K.; Investigation: V.P., C.V., B.Z., C.D., S.C., A.B.F. and O.K.; Methodology: V.P., T.D., C.V., B.Z., C.D. and S.C.; Project administration: V.P., A.B.F. and O.K.; Resources: C.D., S.C., A.B.F. and O.K.; Software: O.K.; Supervision: A.B.F. and O.K.; Validation: T.C. and O.K.; Visualization: V.P. and O.K.; Writing – original draft: V.P., A.B.F. and O.K.; Writing - review & editing: V.P., T.C., T.D., C.V., B.Z., C.D., S.C., A.B.F. and O.K.;

The authors would like to acknowledge the Metabolomics Core Facility at the Institute of Physiology of the Czech Academy of Sciences for lipidomics profiling.

Supplementary Information

PDB and details

10 LITERATURE

1. Birben, E., et al., *Oxidative stress and antioxidant defense*. World Allergy Organ J, 2012. **5**(1): p. 9-19.DOI: 10.1097/WOX.0b013e3182439613
2. Kang, S.W., I.C. Baines, and S.G. Rhee, *Characterization of a mammalian peroxiredoxin that contains one conserved cysteine*. J Biol Chem, 1998. **273**(11): p. 6303-11.DOI: 10.1074/jbc.273.11.6303
3. Zhou, S., et al., *Peroxiredoxin 6 homodimerization and heterodimerization with glutathione S-transferase pi are required for its peroxidase but not phospholipase A2 activity*. Free Radic Biol Med, 2016. **94**: p. 145-56.DOI: 10.1016/j.freeradbiomed.2016.02.012
4. Fisher, A.B., et al., *Inhibition of Peroxiredoxin 6 PLA2 Activity Decreases Oxidative Stress and the Severity of Acute Lung Injury in the Mouse Cecal Ligation and Puncture Model*. Antioxidants (Basel), 2021. **10**(11).DOI: 10.3390/antiox10111676
5. Li, D.X., et al., *Antioxidant protein peroxiredoxin 6 suppresses the vascular inflammation, oxidative stress and endothelial dysfunction in angiotensin II-induced endotheliocyte*. Gen Physiol Biophys, 2020. **39**(6): p. 545-555.DOI: 10.4149/gpb_2020029
6. Wang, X., et al., *Peroxiredoxin 6 knockout aggravates cecal ligation and puncture-induced acute lung injury*. Int Immunopharmacol, 2019. **68**: p. 252-258.DOI: 10.1016/j.intimp.2018.12.053
7. Novoselova, E.G., et al., *Role of Innate Immunity and Oxidative Stress in the Development of Type 1 Diabetes Mellitus. Peroxiredoxin 6 as a New Anti-Diabetic Agent*. Biochemistry (Mosc), 2021. **86**(12): p. 1579-1589.DOI: 10.1134/S0006297921120075
8. Bumanlag, E., E. Scarlata, and C. O'Flaherty, *Peroxiredoxin 6 Peroxidase and Ca(2+)-Independent Phospholipase A2 Activities Are Essential to Support Male-Mouse Fertility*. Antioxidants (Basel), 2022. **11**(2).DOI: 10.3390/antiox11020226
9. Xu, J., et al., *Differential Expression And Effects Of Peroxiredoxin-6 On Drug Resistance And Cancer Stem Cell-Like Properties In Non-Small Cell Lung Cancer*. Onco Targets Ther, 2019. **12**: p. 10477-10486.DOI: 10.2147/OTT.S211125
10. Xu, X., et al., *The phospholipase A2 activity of peroxiredoxin 6 promotes cancer cell death induced by tumor necrosis factor alpha in hepatocellular carcinoma*. Mol Carcinog, 2016. **55**(9): p. 1299-308.DOI: 10.1002/mc.22371
11. Lu, B., et al., *Identification of PRDX6 as a regulator of ferroptosis*. Acta Pharmacol Sin, 2019. **40**(10): p. 1334-1342.DOI: 10.1038/s41401-019-0233-9
12. Fisher, A.B., *Peroxiredoxin 6 in the repair of peroxidized cell membranes and cell signaling*. Arch Biochem Biophys, 2017. **617**: p. 68-83.DOI: 10.1016/j.abb.2016.12.003
13. Fisher, A.B., et al., *A novel lysophosphatidylcholine acyl transferase activity is expressed by peroxiredoxin 6*. J Lipid Res, 2016. **57**(4): p. 587-96.DOI: 10.1194/jlr.M064758
14. Hall, A., et al., *Structure-based insights into the catalytic power and conformational dexterity of peroxiredoxins*. Antioxid Redox Signal, 2011. **15**(3): p. 795-815.DOI: 10.1089/ars.2010.3624
15. Ralat, L.A., et al., *Direct evidence for the formation of a complex between 1-cysteine peroxiredoxin and glutathione S-transferase pi with activity changes in both enzymes*. Biochemistry, 2006. **45**(2): p. 360-72.DOI: 10.1021/bi0520737
16. Chen, J.W., et al., *1-Cys peroxiredoxin, a bifunctional enzyme with glutathione peroxidase and phospholipase A2 activities*. J Biol Chem, 2000. **275**(37): p. 28421-7.DOI: 10.1074/jbc.M005073200
17. Fisher, A.B., et al., *Phospholipid hydroperoxides are substrates for non-selenium glutathione peroxidase*. J Biol Chem, 1999. **274**(30): p. 21326-34.DOI: 10.1074/jbc.274.30.21326
18. Fisher, A.B., et al., *Altered lung phospholipid metabolism in mice with targeted deletion of lysosomal-type phospholipase A2*. J Lipid Res, 2005. **46**(6): p. 1248-56.DOI: 10.1194/jlr.M400499-JLR200

19. Li, H., et al., *Critical role of peroxiredoxin 6 in the repair of peroxidized cell membranes following oxidative stress*. *Free Radic Biol Med*, 2015. **87**: p. 356-65.DOI: 10.1016/j.freeradbiomed.2015.06.009
20. Manevich, Y., et al., *Structure and phospholipase function of peroxiredoxin 6: identification of the catalytic triad and its role in phospholipid substrate binding*. *J Lipid Res*, 2007. **48**(10): p. 2306-18.DOI: 10.1194/jlr.M700299-JLR200
21. Kuda, O., et al., *Nrf2-Mediated Antioxidant Defense and Peroxiredoxin 6 Are Linked to Biosynthesis of Palmitic Acid Ester of 9-Hydroxystearic Acid*. *Diabetes*, 2018. **67**(6): p. 1190-1199.DOI: 10.2337/db17-1087
22. Yore, M.M., et al., *Discovery of a class of endogenous mammalian lipids with anti-diabetic and anti-inflammatory effects*. *Cell*, 2014. **159**(2): p. 318-32.DOI: 10.1016/j.cell.2014.09.035
23. Aryal, P., et al., *Distinct biological activities of isomers from several families of branched fatty acid esters of hydroxy fatty acids (FAHFAs)*. *J Lipid Res*, 2021. **62**: p. 100108.DOI: 10.1016/j.jlr.2021.100108
24. Brejchova, K., et al., *Understanding FAHFAs: From structure to metabolic regulation*. *Prog Lipid Res*, 2020. **79**: p. 101053.DOI: 10.1016/j.plipres.2020.101053
25. Manevich, Y., et al., *Binding of peroxiredoxin 6 to substrate determines differential phospholipid hydroperoxide peroxidase and phospholipase A(2) activities*. *Arch Biochem Biophys*, 2009. **485**(2): p. 139-49.DOI: 10.1016/j.abb.2009.02.008
26. Kagan, V.E., et al., *Oxidized arachidonic and adrenic PEs navigate cells to ferroptosis*. *Nat Chem Biol*, 2017. **13**(1): p. 81-90.DOI: 10.1038/nchembio.2238
27. Fisher, A.B., et al., *A competitive inhibitor of phospholipase A2 decreases surfactant phosphatidylcholine degradation by the rat lung*. *Biochem J*, 1992. **288 (Pt 2)**: p. 407-11.DOI: 10.1042/bj2880407
28. Feinstein, S.I., *Mouse Models of Genetically Altered Peroxiredoxin 6*. *Antioxidants (Basel)*, 2019. **8**(4).DOI: 10.3390/antiox8040077
29. Kuda, O., et al., *Docosahexaenoic Acid-Derived Fatty Acid Esters of Hydroxy Fatty Acids (FAHFAs) With Anti-inflammatory Properties*. *Diabetes*, 2016. **65**(9): p. 2580-90.DOI: 10.2337/db16-0385
30. Paluchova, V., et al., *Triacylglycerol-Rich Oils of Marine Origin are Optimal Nutrients for Induction of Polyunsaturated Docosahexaenoic Acid Ester of Hydroxy Linoleic Acid (13-DHAHLA) with Anti-Inflammatory Properties in Mice*. *Mol Nutr Food Res*, 2020. **64**(11): p. e1901238.DOI: 10.1002/mnfr.201901238
31. Brezinova, M., et al., *Exercise training induces insulin-sensitizing PAHSAs in adipose tissue of elderly women*. *Biochim Biophys Acta Mol Cell Biol Lipids*, 2020. **1865**(2): p. 158576.DOI: 10.1016/j.bbalip.2019.158576
32. Cajka, T., J.T. Smilowitz, and O. Fiehn, *Validating Quantitative Untargeted Lipidomics Across Nine Liquid Chromatography-High-Resolution Mass Spectrometry Platforms*. *Anal Chem*, 2017. **89**(22): p. 12360-12368.DOI: 10.1021/acs.analchem.7b03404
33. Lopes, M., et al., *Metabolomics atlas of oral 13C-glucose tolerance test in mice*. *Cell Rep*, 2021. **37**(2): p. 109833.DOI: 10.1016/j.celrep.2021.109833
34. Dupuy, A., et al., *Simultaneous quantitative profiling of 20 isoprostanooids from omega-3 and omega-6 polyunsaturated fatty acids by LC-MS/MS in various biological samples*. *Anal Chim Acta*, 2016. **921**: p. 46-58.DOI: 10.1016/j.aca.2016.03.024
35. Rund, K.M., et al., *Development of an LC-ESI(-)-MS/MS method for the simultaneous quantification of 35 isoprostanes and isofurans derived from the major n3- and n6-PUFAs*. *Anal Chim Acta*, 2018. **1037**: p. 63-74.DOI: 10.1016/j.aca.2017.11.002
36. Mirdita, M., et al., *ColabFold: making protein folding accessible to all*. *Nat Methods*, 2022. **19**(6): p. 679-682.DOI: 10.1038/s41592-022-01488-1
37. Pettersen, E.F., et al., *UCSF ChimeraX: Structure visualization for researchers, educators, and developers*. *Protein Sci*, 2021. **30**(1): p. 70-82.DOI: 10.1002/pro.3943
38. Chong, J., et al., *MetaboAnalyst 4.0: towards more transparent and integrative metabolomics analysis*. *Nucleic Acids Res*, 2018. **46**(W1): p. W486-W494.DOI: 10.1093/nar/gky310

39. Brejchova, K., et al., *Triacylglycerols containing branched palmitic acid ester of hydroxystearic acid (PAHSA) are present in the breast milk and hydrolyzed by carboxyl ester lipase*. Food Chem, 2022. **388**: p. 132983.DOI: 10.1016/j.foodchem.2022.132983
40. Patel, R., et al., *ATGL is a biosynthetic enzyme for fatty acid esters of hydroxy fatty acids*. Nature, 2022.DOI: 10.1038/s41586-022-04787-x
41. Brejchova, K., et al., *Distinct roles of adipose triglyceride lipase and hormone-sensitive lipase in the catabolism of triacylglycerol estolides*. Proc Natl Acad Sci U S A, 2021. **118**(2).DOI: 10.1073/pnas.2020999118
42. Chowhan, R.K., H. Rahaman, and L.R. Singh, *Structural basis of peroxidase catalytic cycle of human Prdx6*. Sci Rep, 2020. **10**(1): p. 17416.DOI: 10.1038/s41598-020-74052-6
43. Kim, K.H., W. Lee, and E.E. Kim, *Crystal structures of human peroxiredoxin 6 in different oxidation states*. Biochem Biophys Res Commun, 2016. **477**(4): p. 717-722.DOI: 10.1016/j.bbrc.2016.06.125
44. Paluchova, V., et al., *Lipokine 5-PAHSA Is Regulated by Adipose Triglyceride Lipase and Primes Adipocytes for De Novo Lipogenesis in Mice*. Diabetes, 2020. **69**(3): p. 300-312.DOI: 10.2337/db19-0494
45. Tan, D., et al., *Discovery of FAHFA-Containing Triacylglycerols and Their Metabolic Regulation*. J Am Chem Soc, 2019. **141**(22): p. 8798-8806.DOI: 10.1021/jacs.9b00045
46. Riecan, M., et al., *Branched and linear fatty acid esters of hydroxy fatty acids (FAHFA) relevant to human health*. Pharmacol Ther, 2022. **231**: p. 107972.DOI: 10.1016/j.pharmthera.2021.107972
47. Akiba, S., et al., *Characterization of acidic Ca(2+)-independent phospholipase A2 of bovine lung*. Comp Biochem Physiol B Biochem Mol Biol, 1998. **120**(2): p. 393-404.DOI: 10.1016/s0305-0491(98)10046-9
48. Chen, D., et al., *iPLA2beta-mediated lipid detoxification controls p53-driven ferroptosis independent of GPX4*. Nat Commun, 2021. **12**(1): p. 3644.DOI: 10.1038/s41467-021-23902-6
49. Jarc, E. and T. Petan, *A twist of FATE: Lipid droplets and inflammatory lipid mediators*. Biochimie, 2020. **169**: p. 69-87.DOI: 10.1016/j.biochi.2019.11.016